HNUE JOURNAL OF SCIENCE
Natural Sciences 2025, Volume 70, Issue 2, pp. 102-110
This paper is available online at http://hnuejs.edu.vn/ns
DOI: 10.18173/2354-1059.2025-0025

EFFECTS OF MUTATIONS AT POSITION 161 ON FLUORESCENCE LOSS IN mCHERRY

Bui Thi Yen Hang
Faculty of Chemistry, Hanoi National University of Education, Hanoi city, Vietnam
Corresponding author: Bui Thi Yen Hang, email: hangbty@hnue.edu.vn

Received May 5, 2025. Revised May 12, 2025. Accepted June 30, 2025.

Abstract. mCherry is among the most widely used red fluorescent proteins in advanced imaging techniques. However, recent studies have revealed that mCherry and its variants are susceptible to spontaneous degradation, leading to a gradual loss of fluorescence over time. In this study, six mCherry variants were engineered, each featuring a single amino acid mutation at position 161, to investigate the role of this residue in mCherry fluorescence stability. Spectroscopic analysis demonstrated that these substitutions had variable effects on fluorescence retention. Notably, the substitution of Ile161 with Ser, Thr, and Gly resulted in a pronounced loss of fluorescence, whereas replacement with Ala, Val, and Cys produced milder effects. These findings underscore the critical role of residue 161 in chromophore stability in red fluorescent proteins, offering valuable suggestions for designing more stable mCherry variants. Furthermore, preliminary crystallization trials identified promising conditions for future optimization and structural studies, which may elucidate the molecular basis of substitution influence at position 161 on fluorescence stability in mCherry variants.

Keywords: fluorescent proteins, mCherry, chromophore degradation, and crystal structures.

1. Introduction

Fluorescent proteins (FPs) are crucial tools in molecular bioimaging [1], [2]. Over time, numerous FPs have been engineered to significantly enhance their photophysical properties and performance compared to their native forms [3]. The broad range of emission spectra and diverse photophysical characteristics of FPs have facilitated their application in various advanced imaging techniques [4], [5]. Reversibly switchable fluorescent proteins (rsFPs), which can be switched multiple times between fluorescent "on" and non-fluorescent "off" states, have attracted lots of worldwide attention due to their potential in super-resolution imaging applications [6]-[8]. Particularly, red rsFPs, which emit fluorescence within the red wavelength, are promising candidates for dual-color super-resolution microscopy when paired with green rsFPs [9], [10]. Despite their

potential, many currently available red rsFPs exhibit suboptimal photophysical properties, limiting their effectiveness in super-resolution microscopy. Red-emitting rsFPs generally display reduced brightness, prolonged maturation times, or incomplete maturation compared to their green or yellow counterparts [11], [12].

Among the first red-emitting rsFPs developed, rsCherry (also referred to as mCherry_E144V_I161S_F177V_W178F) is a reversibly photoswitchable variant of mCherry, a well-known fluorescent protein [11], [13]. rsCherry exhibits several notable limitations, including low brightness, poor photostability, and a limited contrast between its "on" and "off" states. Moreover, these rsFPs undergo changes in quantum yield rather than a shift in absorption spectra during photoswitching, which complicates their interpretation and modulation [11], [14].

Previous studies have demonstrated that the chromophore in mCherry adopts a *cis*-configuration and appears unable to isomerize to the *trans*-conformation due to steric hindrance from a bulky isoleucine residue at position 161 [13]. When Ser, a smaller amino acid, is replaced with Ile161, the chromophore is capable of adopting a *trans*-configuration, thereby enabling the protein to switch between two configurations corresponding to the fluorescent “on” and non-fluorescent “off” states [11], [15]. However, our previous study has identified an unexpected oxygen-induced chromophore degradation, resulting in irreversible fluorescence loss in mCherry and its derivatives. This phenomenon was found to be strongly related to the mutation Ile161 to Ser [15]. Building on these findings, the present study aims to examine the influence of amino acid mutations at position 161 on the fluorescence loss caused by chromophore degradation in mCherry with the goal of developing more stable, switchable variants in the future.

2. Content

2.1. Experiments

2.1.1. Mutagenesis, protein expression, and purification

The mCherry gene was sourced from Addgene and inserted into pRSETb plasmids between the *BamHI* and *EcoRI* restriction sites (Table 1). The mutants of mCherry were constructed by introducing mutations I161A, I161C, I161G, I161S, I161V or I161T into mCherry using a modified QuikChange protocol [16]. Primers for mutagenesis were designed using the QuikChange Primer Design Tool (Agilent Technologies) and synthesized by Integrated DNA Technologies (IDT).

Table 1. List of used primers

Name of primer	Primer sequence
mCherry_I161A_forward	CCTGAAGGGCGAGGCCAAGCAGAGGCT
mCherry_I161C_forward	CCTGAAGGGCGAGTGCAAGCAGAGGCT
mCherry_I161G_forward	CCTGAAGGGCGAGGGCAAGCAGAGGCT
mCherry_I161V_forward	CCTGAAGGGCGAGGTCAAGCAGAGGCT
mCherry_I161T_forward	CCTGAAGGGCGAGACCAAGCAGAGGCT
mCherry_I161S_forward	CCTGAAGGGCGAGAGCAAGCAGAGGCT

All mCherry mutants were expressed and purified using a consistent protocol. Firstly, the plasmids encoding the desired constructs were subsequently transformed into *E. coli* JM109(DE3) cells via a heat shock method. Following incubation at 21 °C with vigorous shaking for 48 - 72 hours, visibly red cells were collected. The cells were resuspended in a buffer containing 100 mM Tris-HCl, 300 mM NaCl, pH 7.4, and disrupted using a French press. Following centrifugation, the supernatant was incubated with Ni-NTA agarose at 4 °C for 40 minutes. His-tag purification was performed using wash and elution buffers, consisting of a Tris-HCl/NaCl buffer at pH 7.4 containing 20 mM imidazole and 250 mM imidazole, respectively. Size exclusion chromatography was then carried out on a Superdex 200 Increase 10/300 GL column (GE Healthcare), connected to an AKTA Prime system. The elution buffer consisted of 10 mM Tris-HCl and 30 mM NaCl at pH 7.4. The purified protein was concentrated to approximately 10 mg/mL using a Vivaspin 6 3000 MWCO PES ultrafiltration membrane (Sartorius). Protein concentration was determined using a Nanodrop spectrophotometer, and the purified proteins were stored at 4°C for future experiments.

2.1.2. Spectroscopy experiments studying the time-dependent degradation in mCherry mutants

For time-course spectroscopic measurement under standard conditions, protein samples were diluted in buffer containing 100 mM Tris-HCl and 300 mM NaCl, pH 7.4, and incubated at 37 °C. Absorption and fluorescence spectra were measured for samples at different time intervals using a Lambda 950 spectrophotometer (Perkin Elmer) and an FLS980 fluorometer (Edinburgh Instruments), respectively.

2.1.3. Protein crystallization

The crystals of mCherry mutants were grown at 21 °C by the vapor diffusion method under normal air at the Biomolecular Architecture laboratory, KU Leuven, Belgium. Several 96-condition crystallization screens were used to identify initial crystallization conditions for crystal growth. The crystals of some mCherry mutants were obtained by the sitting vapor diffusion method, after a few days to a few weeks, depending on the expressed protein constructs. Prior to X-ray data collection, crystals were transferred into a cryoprotectant solution of identical composition to the mother liquors, supplemented with 20% (*v*/*v*) glycerol and flash-cooled in liquid nitrogen.

2.2. Results and discussion

2.2.1. Generation of mCherry_I161X mutants

The amino acids chosen to replace Ile161 include Ala, Cys, Gly, Ser, Thr, and Val are all smaller than Ile, to create space to allow the chromophore to switch between two states. Six mCherry mutants with a single mutation at position 161, including mCherry_I161A, mCherry_I161C, mCherry_I161G, mCherry_I161S, mCherry_I161V, and mCherry_I161T, were successfully constructed using site-directed mutagenesis. The presence of the intended mutation was confirmed by DNA sequencing. All mutant proteins were expressed and purified, yielding strongly colored solutions. Their absorbance and fluorescence spectra were recorded and are shown in Figure 1.

Overall, none of the mutations resulted in a shift in either emission spectra relative to wild-type *mCherry*, with all variants exhibiting a maximum absorbance at 589 nm and fluorescence emission at 610 nm.

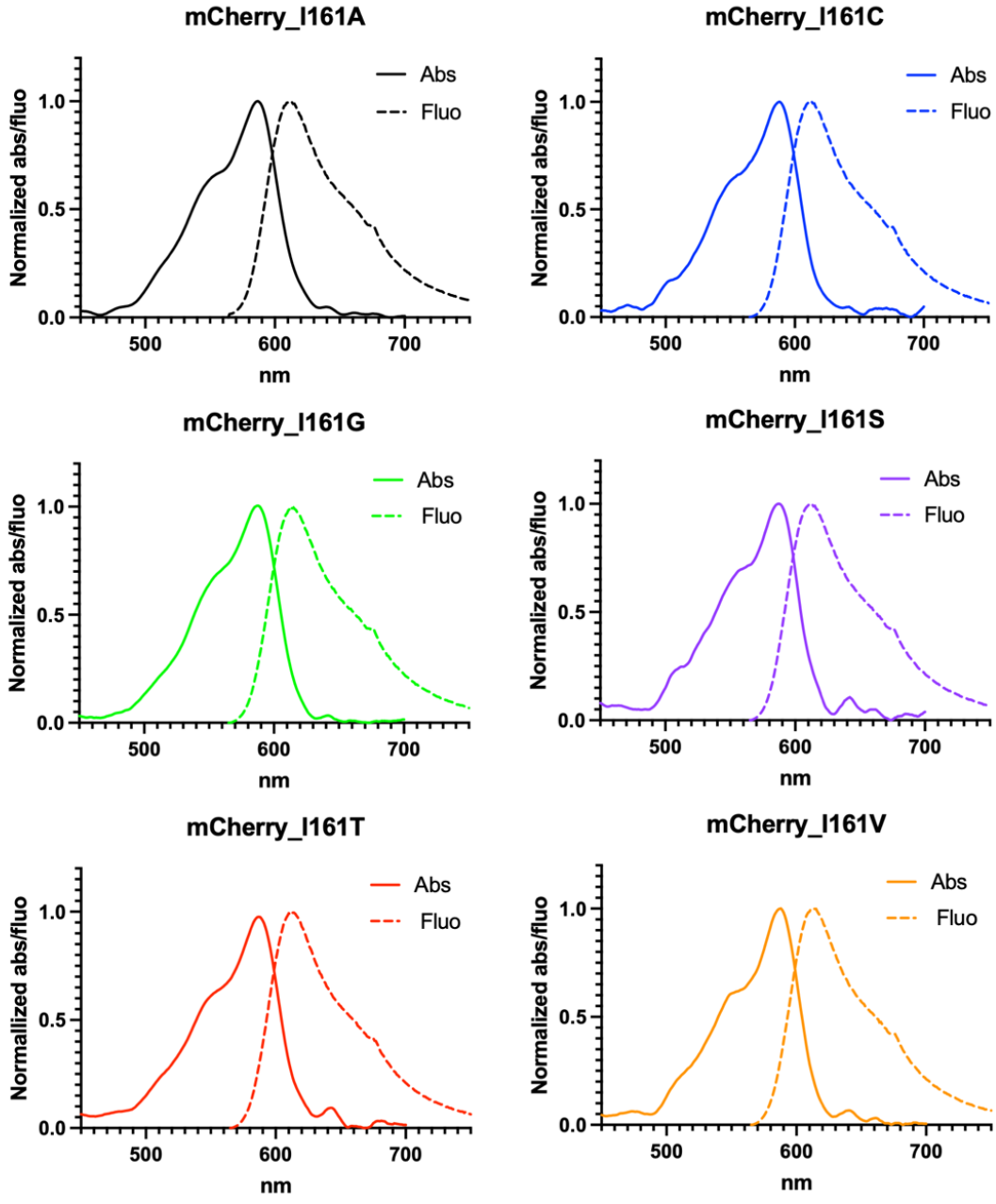

Figure 1. Normalized absorbance (solid lines) and fluorescence (dashed lines) spectra of mCherry mutants. The excitation wavelength for all mutants is fixed at 560 nm

2.2.2. mCherry mutants lose color spontaneously under normal air

mCherry mutants were purified after recombinant bacterial expression to obtain bright red proteins in solution. The mCherry mutants' absorbance and fluorescence loss were accelerated when incubating the sample at 37 °C, following a single exponential decay rate as presented in Figure 2.

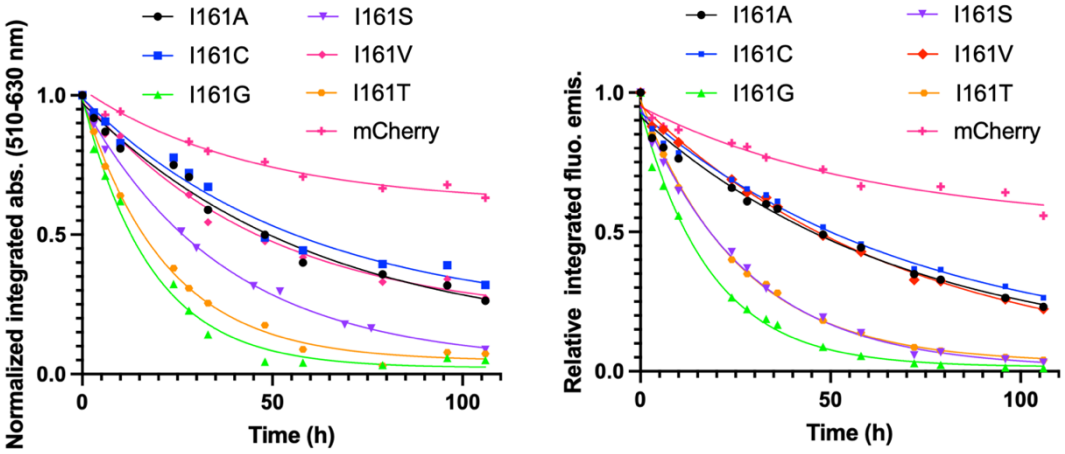

Figure 2. Time-dependent values of normalized integrated absorption 510 - 630 nm (left) and relative integrated fluorescence emission (right) of purified mCherry and its mutants incubated at 37 °C. The lines correspond to single exponential fittings of the absorbance/fluorescence decay

Spectroscopic data clearly indicate that all mutations (Ala, Cys, Gly, Ser, Thr, or Val) introduced to position 161 accelerate the loss of both fluorescence and absorbance, but to different extents. These results strongly support the hypothesis that the bulky, hydrophobic nature of the Ile side chain plays a protective role, likely by sterically hindering configurational changes between *cis*- and *trans*-, or limiting access of oxygen to the chromophore environment (Figure 3). Intriguingly, the loss of fluorescence and maximum absorbance peaks becomes vigorous when Ile161 is substituted by Thr, Ser, Gly; meanwhile, the effect of replacing I161 by Ala, Val, or Cys is milder (Figure 2). It is noted that Ser, Thr are polar side chains containing hydroxyl groups, while Gly, with the absence of a side chain, would provide the largest space for chromophore flexibility. This suggests that increased flexibility or polarity in the vicinity of the chromophore, afforded by these smaller residues, might destabilize the chromophore or facilitate the chemical reactions leading to its degradation. Conversely, substitutions with Ala, Val, and Cys resulted in a milder acceleration of degradation compared to Ser/Thr/Gly. Ala and Val maintain hydrophobicity but are less bulky than Ile, while Cys introduces a unique thiol group. The obtained results suggest that maintaining some degree of hydrophobicity and/or moderate steric bulk at position 161 is preferable to introducing highly flexible or polar residues.

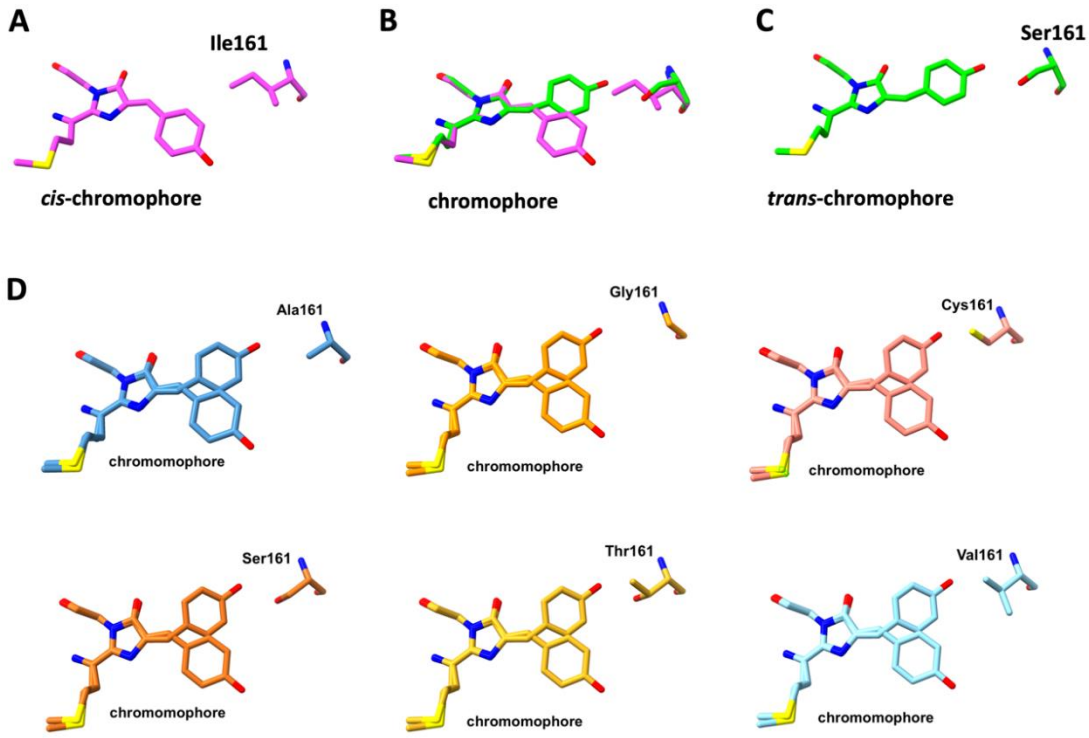

Figure 3. (A) cis-chromophore in mCherry (PDB code: 2h5q [13]), (B) superimposition of the two structures of rsCherry and mCherry; (C) trans-chromophore in rsCherry (PDB code: 8b65 [15]), and (D) the proposed structures of mCherry mutants with Ala161, Gly161, Cys161, Ser161, Thr161, or Val161.
Carbon atoms in the mCherry and rsCherry are colored green and magenta, respectively. Oxygen, nitrogen, and sulfur atoms are colored red, blue, and yellow, respectively

2.2.3. Protein crystallization

The crystals of mCherry_I161A, mCherry_I161C, mCherry_I161S, mCherry_I161V, and mCherry_I161T were obtained within about two weeks. The crystallization conditions producing crystals and the crystal images are presented in Table 2 and Figure 4, respectively. Some crystals retained their bright red color (mCherry_I161A, mCherry_I161C, mCherry_I161T), while crystals of mCherry_I161S and mCherry_I161T lost their color. These observations are consistent with the measured spectroscopic data of these proteins in solutions (Figure 2). The chromophore degradation, which results in fluorescence loss in these mCherry mutants, might partially explain the difficulties in obtaining well-diffracting crystals. Despite some growing crystals, these obtained crystals diffracted badly, and no usable X-ray diffraction data were collected. Therefore, Further optimization will be required to improve the crystallization quality of these mCherry mutants.

Table 2. Crystallization conditions

Protein	Crystallization cocktails
mCherry_I161A	0.1 M Sodium HEPES pH 7.5, 25% w/v PEG 6000
mCherry_I161C	0.1 M Sodium HEPES pH 7.5, 25% w/v PEG 6000
mCherry_I161S	0.2 M Sodium acetate, 20% w/v PEG 3350
mCherry_I161V	0.1 M Sodium acetate pH 4.6, 20% w/v PEG 10000
mCherry_I161T	0.1 M Sodium HEPES pH 7.5, 25% w/v PEG 6000

PEG: Polyethylene glycol, HEPES: (4-(2-hydroxyethyl)-1-piperazineethanesulfonic acid)

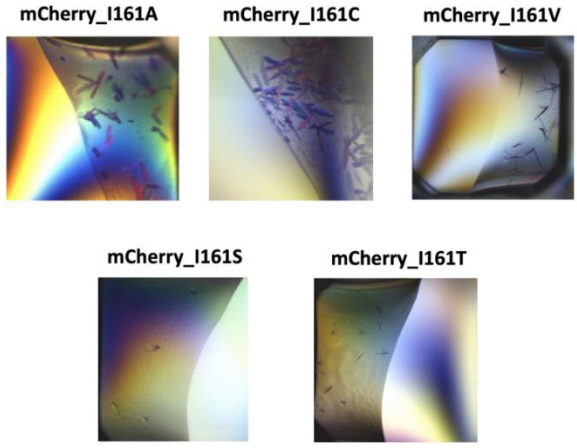

Figure 4. Images of some obtained crystals for mCherry_161A, mCherry_161C, mCherry_161S, mCherry_161V and mCherry_161T

3. Conclusions

In this study, six mCherry mutants with only different amino acid substitutions at position 161 were successfully generated and confirmed by DNA sequencing. Spectroscopic analyses revealed that these mutants exhibit varying rates of fluorescence loss under normal air, indicating differences in their sensitivity to fluorescence loss. The Ile161 was demonstrated to provide significant protection to the chromophore; therefore, substitutions of Ile161 led to varying degrees of accelerated degradation. Specifically, mutations from the original Ile161 to Ser, Thr, or Gly led to a pronounced loss of fluorescence, whereas changes to Ala, Val, or Cys resulted in less severe effects. These results deepen our understanding of red fluorescent protein chromophore stability and offer valuable empirical data to guide the rational design of more photostable red fluorescent proteins for advanced bioimaging applications. Additionally, initial crystallization trials led to the successful growth of crystals for several mutants, providing a promising suggestion for future structural analysis. However, further studies are required to obtain crystal structures of these mCherry mutants and fully elucidate the mechanism of oxygen-induced degradation in mCherry variants.

Acknowledgments. The study is supported by grants from the Hanoi National University of Education (Project SPHN24-05).

REFERENCES

[1] Chudakov DM, Lukyanov S & Lukyanov KA, (2005). Fluorescent proteins as a toolkit for *in vivo* imaging. *Trends in Biotechnology*, 23(11), 605-613. DOI: 10.1016/j.tibtech.2005.10.005.

[2] Chudakov D, Matz M, Lukyanov S & Lukyanov K, (2010). Fluorescent proteins and their applications in imaging living cells and tissues. *Physiological Reviews*, 90(3), 1103-1163. DOI: 10.1152/physrev.00038.2009.

[3] Rodriguez EA, Campbell RE, Lin JY, Lin MZ, Miyawaki A, Palmer AE, Shu X, Zhang J & Tsien RY, (2017). The growing and glowing toolbox of fluorescent and photoactive proteins. *Trends in Biochemical Sciences*, 42(2), 111-129. DOI: 10.1016/j.tibs.2016.09.010.

[4] Jing Y, Zhang C, Yu B, Lin D & Qu J, (2021). Super-resolution microscopy: Shedding new light on *in vivo* imaging. *Frontiers in Chemistry*, 9, 746900. DOI: 10.3389/fchem.2021.746900.

[5] Lu K, Vu CQ, Matsuda T & Nagai T, (2019). Fluorescent protein-based indicators for functional super-resolution imaging of biomolecular activities in living cells. *International Journal of Molecular Sciences*, 20(22), 5784. DOI: 10.3390/ijms20225784.

[6] Bourgeois D & Adam V, (2012). Reversible photoswitching in fluorescent proteins: A mechanistic view. *IUBMB Life*, 64(6), 482-491. DOI: 10.1002/iub.1023.

[7] Nienhaus K & Nienhaus GU, (2016). Photoswitchable fluorescent proteins: Do not always look on the bright side. *ACS Nano*, 10(10), 9104-9108. DOI: 10.1021/acsnano.6b06298.

[8] Tang L & Fang C, (2022). Photoswitchable fluorescent proteins: Mechanisms on ultrafast timescales. *International Journal of Molecular Sciences*, 23(12), 6459. DOI: 10.3390/ijms23126459.

[9] Andresen M, Stiel AC, Fölling J, Wenzel D, Schönle A, Egner A, Eggeling C, Hell SW & Jakobs S, (2008). Photoswitchable fluorescent proteins enable monochromatic multilabel imaging and dual color fluorescence nanoscopy. *Nature Biotechnology*, 26(9), 1035-1040. DOI: 10.1038/nbt.1493.

[10] Siegel A, Baird M, Davidson M & Day R, (2013). Strengths and weaknesses of recently engineered red fluorescent proteins evaluated in live cells using fluorescence correlation spectroscopy. *International Journal of Molecular Sciences*, 14(10), 20340-20358. DOI: 10.3390/ijms141020340.

[11] Stiel AC, Andresen M, Bock H, Hilbert M, Schilde J, Schönle A, Eggeling C, Egner A, Hell SW & Jakobs S, (2008). Generation of monomeric reversibly switchable red fluorescent proteins for far-field fluorescence nanoscopy. *Biophysical Journal*, 95(6), 2989-2997. DOI: 10.1529/biophysj.108.130146.

[12] Shcherbakova DM, Subach OM & Verkhusha VV, (2012). Red fluorescent proteins: advanced imaging applications and future design. *Angewandte Chemie International Edition*, 51(43), 10724-10738. DOI: 10.1002/anie.201200408.

[13] Shu X, Shaner NC, Yarbrough CA, Tsien RY & Remington SJ, (2006). Novel chromophores and buried charges control color in *m*fruits. *Biochemistry*, 45(32), 9639-9647. DOI: 10.1021/bi0607731.

[14] Subach FV, Malashkevich VN, Zencheck WD, Xiao H, Filonov GS, Almo SC & Verkhusha VV, (2009). Photoactivation mechanism of PAmCherry based on crystal structures of the protein in the dark and fluorescent states. *Proceedings of the National Academy of Sciences of the United States of America*, 106(50), 21097-21102. DOI: 10.1073/pnas.0909204106.

[15] Bui TYH, De Zitter E, Moeyaert B, Pecqueur L, Srinivasu BY, Economou A, Fontecave M, Van Meervelt L, Dedecker P & Pedre B, (2023). Oxygen-induced chromophore degradation in the photoswitchable red fluorescent protein rsCherry. *International Journal of Biological Macromolecules*, 239, 124179. DOI: 10.1016/j.ijbiomac.2023.124179.

[16] Duwé S, De Zitter E, Gielen V, Moeyaert B, Vandenberg W, Grotjohann T, Clays K, Jakobs S, Van Meervelt L & Dedecker P, (2015). Expression-enhanced fluorescent proteins based on enhanced green fluorescent protein for super-resolution microscopy. *ACS Nano*, 9(9), 9528-9541. DOI: 10.1021/acsnano.5b04129.